Modeling the light-induced degradation (LID) in silicon due to A_{Si}-Si_i-defects

K. Lauer[1,2], A. Flötotto[1], D. Bratek[1], R. Müller[1], K. Peh[1], D. Schulze[1], W.J.D. Beenken[1] and S. Krischok[1]

[1]TU Ilmenau, Institut für Physik und Institut für Mikro- und Nanotechnologien

kevin.lauer@tu-ilmenau.de

[2]CiS Forschungsinstitut für Mikrosensorik GmbH

klauer@cismst.de

Abstract

Light-induced degradation (LID) in silicon is one of the major problems that hamper the progress in silicon solar cell technology. We present a method to model the LID kinetics by a differential equation system based on the assumption of charge-state-change-induced configuration changes of the so-called A_{Si}-Si_i-defect. Assuming realistic transition rates, we solve this differential equation system under variation of some of the transition rates. It is found that the LID kinetics can in principle be modeled by this approach but care has to be taken if transition rates put into the model are directly extracted from time-dependent carrier lifetime measurements.

1 Introduction

Silicon is the material which can be produced by mankind with the highest purity of all mass-produced materials so far. Its high purity allows the manufacturing of such important devices like computers, mobile phones or most importantly solar cells. Therefore, it is remarkable that despite all the knowledge on silicon physics and technology gained over the last about 70 years this material is still insufficiently understood. A technologically and economically example is the phenomenon of light-induced degradation (LID) in silicon solar cells,[1] which hampered the progress in solar cell development for years.

A decade ago a possible mechanism of LID in silicon based on the so-called A_{Si}-Si_i-defect model was proposed.[2] A thorough recent review of the A_{Si}-Si_i-defect model and

its implications on so far generally accepted interpretations of experimental data related to defects in silicon, as well as alternative explanations provides Ref. [3].

The term "A_{Si}-Si$_i$-defect" refers to an acceptor A atom on or near a Si site very close to an 'interstitial' Si atom. Early ideas of such defect complexes were put forward by Wever et al.[4] initiating a C_{Si}-Si$_i$-defect as origin for the photoluminescence G line in silicon, which shows well pronounced meta stabilities. Meta-stable behavior results often from charge-induced defect configuration changes. Thanks serendipity we were able to develop a comprehensive model for the LID phenomenon. Within this model the transitions between defect states are assumed to be of first order kinetics. This is in line with reported data [5]–[8] on this defect, which always assume the simplest case namely first order kinetics for the reactions behind the LID phenomenon. In this contribution, we show how the time-evolution of the LID phenomenon in Si can be modeled within A_{Si}-Si$_i$-defect model by solving a system of linear differential equations describing the transitions between seven A_{Si}-Si$_i$-defect states.

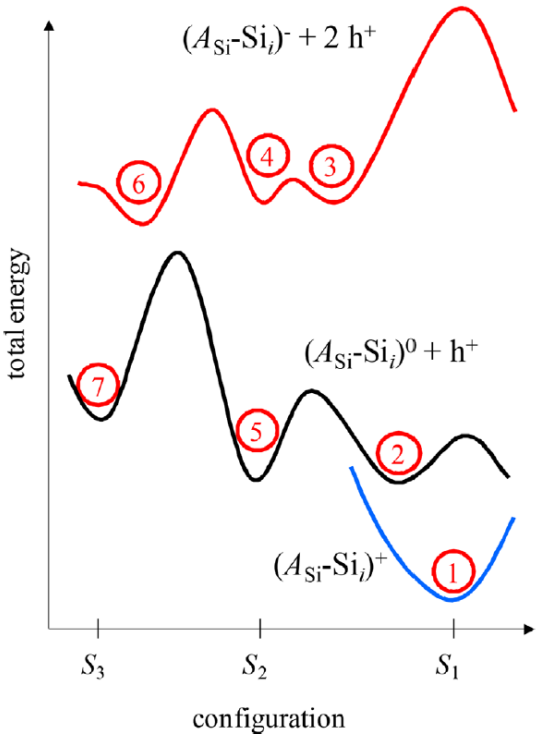

Fig. 1: Schematically configuration coordinate-energy (cc) diagram of the A_{Si}-Si$_i$-defect model with seven states and 16 possible transitions, after Ref. [9]

2 Theoretical background

In *Fig. 1* the configuration coordinate-energy (cc) diagram of the A_{Si}-Si_i-defect model is replotted from Ref. [9]. Three different atomic configurations denoted by S_1, S_2 and S_3 are assumed to be possible. The A_{Si}-Si_i-defect can be charged positively or negatively or be neutral, which may or may not change the local configurations slightly, which is accounted for by horizontal displacements of the minima positions. Depending on the charge state different defect configurations can be meta-stable and the global minimum may change between them.

Considering forward and backward transitions between neighboring configurations, in the proposed model there are 16 conceivable rates $k_{j\to i}$ in total, which can be partitioned into two categories:

The first category is given by changes of the configuration of the defect without changing the charge. These transitions may be described as motion along a configuration coordinate on a potential energy surface with several activation energy barriers. In our context we will reduce this picture to incoherent hopping processes between the respective potential energy surface minima with rates given by the minimum configuration energies as well as the barrier heights between them. An example for such a transition is that from state 4 to state 6 on the potential energy surface for the negatively charged defect.

The second kind of transitions comprise a change of the defect charge due to capture or ejection of electrons or holes, respectively. According to the Franck Condon approximation, we assume that these transitions are almost vertical, i.e. with only minor changes in the configuration coordinate of the defect. For example, the transition from state 6 to 7 represents a hole capture. With this notation we follow cc-diagrams of the past, where such transitions are indicated as vertical lines.[10] These transitions are not necessarily fluorescent [11] but represent non-radiative multi phonon emission processes. Due to the capture or emission of electrons or holes the determination of the rates requires not only the defect energy as shown *Fig. 1* but also the inclusion of chemical potentials for electrons and holes, respectively. [12] Note that for illumination these differ from each other, namely as quasi-Fermi-levels.

For each transition we assume a constant rate denoted by $k_{j\to i}$. The indices *j* and *i* indicate the minimum configuration states within the A_{Si}-Si_i-defect model, and the arrow the direction of the transition. This means for example that $k_{4\to 6}$ denotes the transition rate from state 4 to state 6. For a discussion of the dependencies of these transition rates on, e.g., the activation energy see Ref. [9].

We assume that all processes are first order reactions. In case of the transitions between states on the same potential energy surface, i.e. $3 \leftrightarrow 4 \leftrightarrow 6$ and $2 \leftrightarrow 5 \leftrightarrow 7$, the linearity is evident, since there is no other reaction partner. The transitions between potential energy surfaces, e.g. $6 \rightarrow 7$, $4 \rightarrow 5$ or $2 \rightarrow 1$, however, are accompanied by hole capture and, therefore, depend on the hole density. Assuming, that this is constant for a given chemical potential, i.e. the holes represent an inexhaustible reservoir due to permanent optical pumping of the band-to-band transitions during illumination, and since the remaining dependences on the defect state concentrations (denoted by $[Z_i]$) is linear, the surface hopping process may be assumed as linear as well. For the reverse transitions $7 \rightarrow 6$, $5 \rightarrow 4$ or $1 \rightarrow 2$, the same arguments hold for capturing electrons, respectively. Now, we can set up a differential equation system for the concentration of defects $[Z_i]$ in different states *i* of the A_{Si}-Si$_i$-defect model [9]:

$$\frac{d[Z_i](t)}{dt} = \sum_{j=1}^{7} k_{j\rightarrow i} \cdot [Z_j](t) \quad \text{with} \quad k_{i\rightarrow i} = -\sum_{j\neq i} k_{i\rightarrow j}. \tag{1}$$

For given transition rates $k_{j\rightarrow i}$ and given initial conditions $[Z_i](t=0)$ the concentration $[Z_i](t)$ for each state *i* of the A_{Si}-Si$_i$-defect can be calculated as a function of time approaching the thermal equilibrium.

Finally, the defect concentrations $[Z_i](t)$ are connected to the measured carrier lifetime by assuming fixed Shockley-Read-Hall (SRH) prefactors for all A_{Si}-Si$_i$-defect configurations.[9]

3 Simulation method

The differential equation system *Eq. (1)* has been solved using the python code which is given in the appendix. To avoid the singularity problem, we solved only six differential equations for the concentrations $[Z_1](t)$ to $[Z_6](t)$ and utilized the continuity equation for $[Z_7](t)$, i.e. $[Z_7] = 1 - \sum_{i=1}^{6}[Z_i]$. For the calculation we normalized all state concentrations to the overall defect concentration.

As an example, the transition rates $k_{j\rightarrow i}$ for LID in boron doped silicon at 40°C are given in *Tab. 1*. The rate $k_{3\rightarrow 4}$ may be identified as the generation rate of the fast LID component (FRC), $k_{4\rightarrow 6}$ as the generation rate for the slow LID component (SRC), $k_{7\rightarrow 5}$ as the annihilation rate of the SRC and $k_{5\rightarrow 2}$ the annihilation rate of the FRC. The values of these rates were estimated from the diagrams published by Bothe and Schmidt.[7] The corresponding back reaction rates for the SRC ($k_{6\rightarrow 4}$ and $k_{5\rightarrow 7}$) are assumed to be

one order of magnitude smaller, whereas the back reaction rates for the FRC ($k_{4\to3}$ and $k_{2\to5}$) appear to be the same as the respective forward reactions. The latter assumption implies that the respective energies of the states, e.g. 3 and 4, are nearly equal in the A_{Si}-Si$_i$-defect model. Finally, all charge-changing transitions ($k_{1\leftrightarrow2}$, $k_{2\leftrightarrow3}$, $k_{4\leftrightarrow5}$, and $k_{6\leftrightarrow7}$) were assumed to be much faster than the configuration changes on the same potential energy surface. Notably, the LID process is quite insensitive to the actual values of these rates, but rather depends on the ratio between electron and hole capture processes. For the illuminated silicon, we set the electron capture rates $k_{1\to2}$, $k_{2\to3}$, $k_{4\to5}$ and $k_{7\to6}$ to 100 s^{-1} and the hole capture rates $k_{2\to1}$, $k_{3\to2}$, $k_{4\to5}$ and $k_{6\to7}$ to 1 s^{-1}, in correspondence to measurements on Fe$_i$ defects in Si.[13] Notably, these rates are only a first guess and we will particularly discuss the effect of varying the most relevant rates $k_{3\to4}, k_{4\to3}$ and $k_{6\to4}$ on the solution of *Eq. (1)* in the next section.

Tab. 1: Matrix of the assumed transition rates $k_{j\to i}$ for the A_{Si}-Si$_i$ defect if A = B = boron, under illumination at 40°C.

		j						
	$k_{j\to i}$ **[1/s]**	1	2	3	4	5	6	7
i	1	$k_{1\to1}$	1	0	0	0	0	0
	2	100	$k_{2\to2}$	1	0	0.027	0	0
	3	0	100	$k_{3\to3}$	0.05	0	0	0
	4	0	0	0.05	$k_{4\to4}$	100	7x10^{-6}	0
	5	0	0.027	0	1	$k_{5\to5}$	0	7x10^{-9}
	6	0	0	0	7x10^{-5}	0	$k_{6\to6}$	100
	7	0	0	0	0	7x10^{-10}	1	$k_{7\to7}$

4 Results

For the B$_{Si}$-Si$_i$-defect, i.e. boron at the substitutional position A_{Si}, the transition rates given in *Tab. 1* result in a solution of *Eq. (1)* as shown in *Fig. 2* for each state Z$_i$. In the

short run, state 3 is populated from state 1 via state 2. Then, the configuration changes from state 3 to 4 until after 100 s an equilibrium has been reached. Then, a slower configuration change from state 4 to 6 takes place until the final equilibrium is reached in the long run.

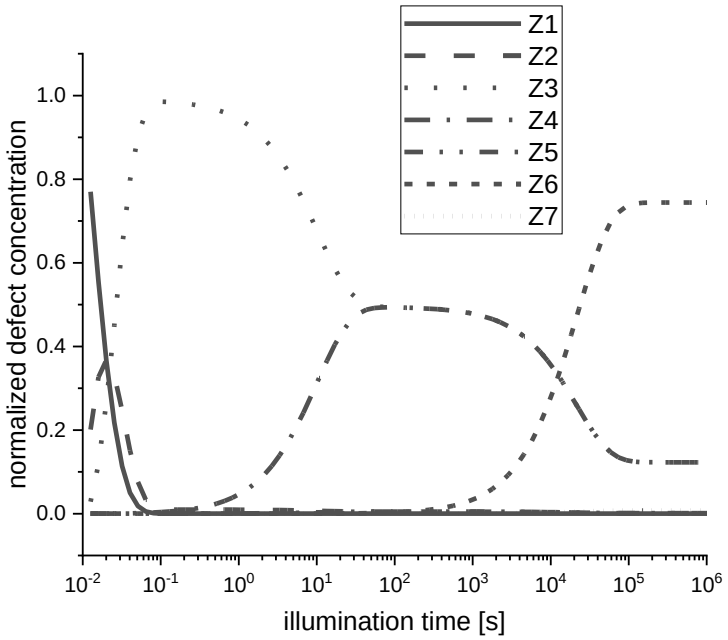

Fig. 2: Normalized defect concentration for all seven states i of the A_{Si}-Si_i-defect as shown in Fig. 1 during illumination. The transition rates used for Eq. (1) are given in Tab. 1.

To transform these normalized defect concentrations into a charge-carrier lifetime, which is finally measured, we multiplied $[Z_4]$ and $[Z_6]$ each with a constant factor as motivated by SRH theory. Since these SRH factors are so far unknown for the A_{Si}-Si_i-defect, we estimated them from lifetime measurements for the initial, the intermediate, and the final stage of the LID process. This allows us to compare our model results with measurements of the carrier lifetime during illumination as shown in *Fig. 3*.

Figure 3 shows two time-scales for carrier lifetime decrease corresponding to the fast component (FRC) and slow component (SRC) of LID. The simulation describes the measured change in the charge-carrier lifetime for the SRC quite well, which indicates that the used transition rate $k_{4\to6}$ of the A_{Si}-Si_i-defect model is a good first approximation for the SRC. The impact of the backward transition rate $k_{6\to4}$ on the measured SRC generation rate will be discussed later.

In contrast, we find that the rate $k_{3\to4}$ directly taken from the FRC of the measured LID [7] in the simulation does not reproduce the experiment. Obviously, the backward transition rate $k_{4\to3}$ has a strong impact. The reader interested in this matter is referred to

the discussion of this problem using more simple defect complexes, namely the A_{Si}-Fe$_i$-defects in Ref. [14].

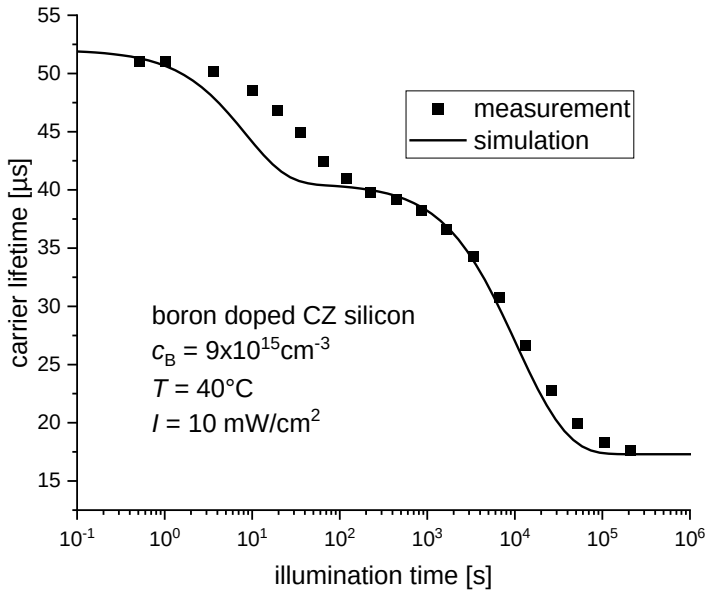

Fig. 3: Comparison of the carrier lifetime measured on a typical boron-doped silicon sample prone to the LID phenomenon with the modeled carrier lifetime based on the solution of Eq. (1) shown in Fig. 2.

To further explore the impact of the transition rates on the modeled charge carrier lifetime and finally the extracted transition rate, we changed systematically the transition rates $k_{3\to4}, k_{4\to3}$ and $k_{6\to4}$ of the A_{Si}-Si$_i$-defect model and solved *Eq. (1)* again. Then, we simulated the lifetime measurement during the LID process and extract from the simulated lifetime curve by fitting a mono-exponential function a simulated transition rate. The simulated transition rate is then compared with the transition rate put into the simulation. These simulated transition rates can be identified with the transition rates, which can be extracted from time-dependent carrier lifetime measurements during LID by a mono-exponential fit if only one defect reaction is assumed.

In *Fig. 4* and *Fig. 5* the simulated evolution of the carrier lifetime is shown for variation of the most relevant rates within the A_{Si}-Si$_i$-defect model $k_{3\to4} = k_{4\to3}$ and $k_{6\to4}$, respectively. The difference between these transition rates which are put into the simulation and the simulated transition rates can be found in *Fig. 4* and *Tab. 2*.

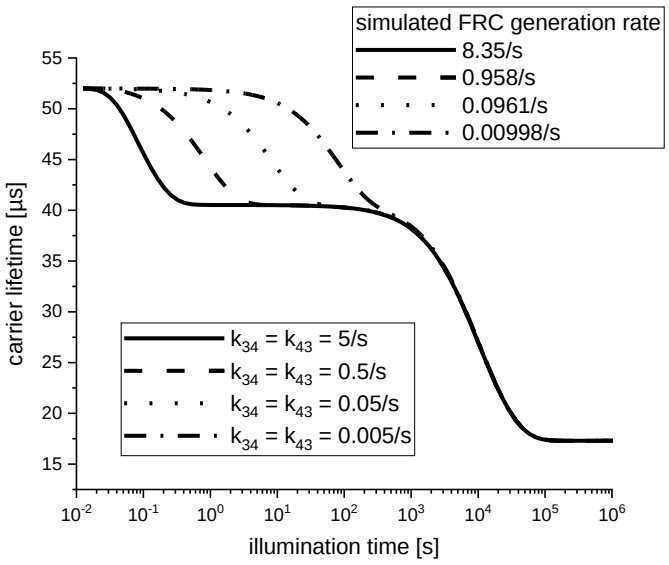

Fig. 4: Modeled carrier lifetime during LID for different transition rates $k_{3\to4} = k_{4\to3}$. Additionally, the simulated FRC transition rate is given in the diagram.

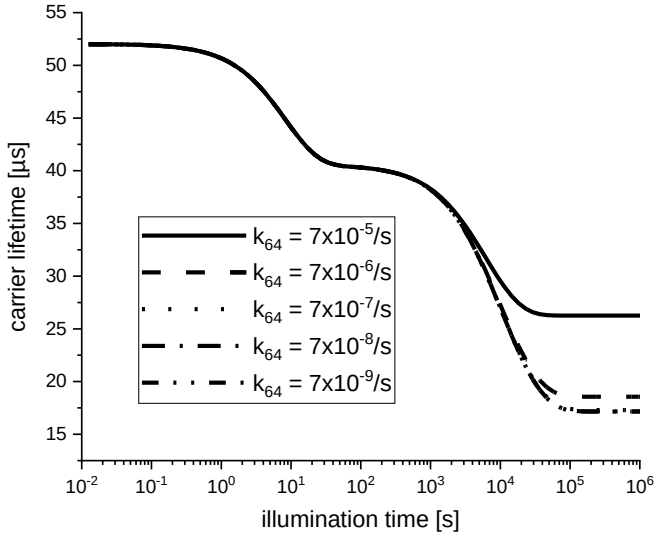

Fig. 5: Modeled carrier lifetime during LID for varying transition rate $k_{6\to4}$.

For the FRC process of LID we find a difference of about a factor of two between the rate put into the simulation and the simulated FRC transition rate. In case of the SRC process of LID we varied the backward transition rate $k_{6\to4}$ while holding the forward transition rate $k_{4\to6}$ constant. The difference between $k_{4\to6}$ and the simulated generation rate of SRC decreases roughly with decreasing $k_{6\to4}$. The largest difference is observed if $k_{4\to6}$ equals $k_{6\to4}$.

Tab. 2: Comparison between the transition rate $k_{4\to6}$ put into the simulation and the simulated transition rate of the SRC while varying the backward transition rate $k_{6\to4}$.

$k_{6\to4}$ put into simulation [1/s]	$k_{4\to6}$ put into simulation [1/s]	simulated generation rate of SRC [1/s]
$7.0 \cdot 10^{-5}$	$7.0 \cdot 10^{-5}$	$1.2 \cdot 10^{-4}$
$7.0 \cdot 10^{-6}$	$7.0 \cdot 10^{-5}$	$5.3 \cdot 10^{-5}$
$7.0 \cdot 10^{-7}$	$7.0 \cdot 10^{-5}$	$4.7 \cdot 10^{-5}$
$7.0 \cdot 10^{-8}$	$7.0 \cdot 10^{-5}$	$4.9 \cdot 10^{-5}$
$7.0 \cdot 10^{-9}$	$7.0 \cdot 10^{-5}$	$4.6 \cdot 10^{-5}$

These investigations exemplify that the simulated transition rates depend in principle on a lot of different transitions in such a complex model like the A_{Si}-Si_i-defect model and sophisticated measurement strategies are necessary to extract transition rates from time-dependent carrier lifetime measurements which can be compared to calculated transition rates.

5 Conclusion

Silicon is one of the most investigated materials on earth. Nevertheless, evrolution in research on some defects in silicon and their kinetics, both in the dark and illuminated, limits the technology development of e.g. inexpensive highly efficient silicon solar cells. In particular, the light-induced degradation (LID) needs to be overcome. In this contribution the A_{Si}-Si_i-defect model is used to explain the kinetics of the LID phenomenon. The LID phenomenon is simulated by a system of linear differential equations based on the A_{Si}-Si_i-defect model assuming charge-state-change-induced configuration changes. The impact of varying transition rates within the model on simulated transition rates is shown and very good fits to the experimentally observed complex LID kinetics are obtained. To get a deeper insight into those configuration changes and corresponding transition rates comprehensive DFT calculations are underway, made by the SimASiSii group at the TU Ilmenau.

Acknowledgement

We thank Erich Runge, TU Ilmenau, Germany, for valuable discussions and thorough proof-reading. This work was supported by the project SimASiSii of the Deutsche Forschungsgemeinschaft (DFG KR 2228/11-1, LA 4623/1-1, RU 1383/6-1, RU 1383/8-1).

Literature

[1] J. Lindroos and H. Savin, 'Review of light-induced degradation in crystalline silicon solar cells', *Sol. Energy Mater. Sol. Cells*, vol. 147, pp. 115–126, Apr. 2016.

[2] C. Möller and K. Lauer, 'Light-induced degradation in indium-doped silicon', *Phys. Status Solidi RRL - Rapid Res. Lett.*, vol. 7, no. 7, pp. 461–464, Jul. 2013.

[3] K. Lauer, K. Peh, D. Schulze, T. Ortlepp, E. Runge, and S. Krischok, 'The ASi–Sii Defect Model of Light-Induced Degradation (LID) in Silicon: A Discussion and Review', *Phys. Status Solidi A*, vol. 219, no. 19, p. 2200099, 2022.

[4] K. Thonke, H. Klemisch, J. Weber, and R. Sauer, 'New model of the irradiation-induced 0.97-eV G line in silicon: A C_{Si}-Si* complex', *Phys. Rev. B*, vol. 24, no. 10, pp. 5874–5886, Nov. 1981.

[5] S. Rein, T. Rehrl, W. Warta, S. Glunz, and G. Willeke, 'Electrical and Thermal Properties of the Metastable Defect in Boron-Doped Czochralski Silicon (Cz-Si)', in *17th European Photovoltaic Solar Energy Conference, WIP Munich*, 2001, p. 1555.

[6] J. Schmidt and K. Bothe, 'Structure and transformation of the metastable boron- and oxygen-related defect center in crystalline silicon', *Phys Rev B*, vol. 69, no. 024107, p. 024107, 2004.

[7] K. Bothe and J. Schmidt, 'Electronically activated boron-oxygen-related recombination centers in crystalline silicon', *J Appl Phys*, vol. 99, p. 013701, 2006.

[8] J. Schmidt and K. Bothe, 'Electronically stimulated degradation of silicon solar cells', *JMatRes*, vol. 21, no. 1, pp. 5–12, 2006.

[9] K. Lauer, C. Möller, C. Tessmann, D. Schulze, and N. V. Abrosimov, 'Activation energies of the In_{Si}-Si_i defect transitions obtained by carrier lifetime measurements', *Phys. Status Solidi C*, vol. 14, no. 5, p. 1600033, 2017.

[10] L. W. Song, X. D. Zhan, B. W. Benson, and G. D. Watkins, 'Bistable interstitial-carbon–substitutional-carbon pair in silicon', *Phys. Rev. B*, vol. 42, no. 9, p. 5765, 1990.

[11] A. Flötotto, 'Tieftemperaturphotolumineszenzspektroskopie (TTPL) und Dichtefunktionaltheorie (DFT) zur weiteren Analyse des A_{Si}-Si_i-Defekts', Nov. 2022, doi: 10.22032/dbt.53715.

[12] A. Alkauskas, M. D. McCluskey, and C. G. V. de Walle, 'Tutorial: Defects in semiconductors—Combining experiment and theory', *J. Appl. Phys.*, vol. 119, no. 18, p. 181101, May 2016.

[13] C. Sun, F. E. Rougieux, and D. Macdonald, ‘A unified approach to modelling the charge state of monatomic hydrogen and other defects in crystalline silicon’, *J. Appl. Phys.*, vol. 117, no. 4, p. 045702, Jan. 2015.

[14] K. Lauer, C. Möller, D. Debbih, M. Auge, and D. Schulze, ‘Determination of activation energy of the iron acceptor pair association and dissociation reaction’, *Solid State Phenom.*, vol. 242, p. 230, Sep. 2015.

Author address

Dr. rer. nat. Kevin Lauer

TU Ilmenau, Institut für Physik und Institut für Mikro- und Nanotechnologien

Weimarer Str. 32

98693 Ilmenau, Germany

Phone: 03677-693758

E-Mail: kevin.lauer@tu-ilmenau.de

CiS Forschungsinstitut für Mikrosensorik GmbH

Konrad-Zuse-Str. 14

99099 Erfurt, Germany

Phone: 0361-6631211

E-Mail: klauer@cismst.de

Appendix

Source code of python program to solve the differential equation system.

```
import numpy as np
import matplotlib.pyplot as plt
from scipy.integrate import odeint
#rates [1/s]
k34 = .05; k43 = .05;
k46 = 7e-5; k64 = 7e-6;
k57 = 7e-10;k75 = 7e-9;
k25 = .027; k52 = .027;

Lon = 100; Loff = 1;
k12 = Lon; k21 = Loff;
k23 = Lon; k32 = Loff;
k45 = Loff; k54 = Lon;
k67 = Loff; k76 = Lon;

#initial conditions
```

```
z10 = 1.0; z20 = 0.0; z30 = 0.0; z40 = 0.0; z50 = 0.0; z60 = 0.0
#number of time steps
tmax = 100
#time steps, logarithmic from 0.01 to 10000000
t = np.logspace(-2,8,tmax)

#definition of DEQ system, 6 coupled DEQ and 1 continuity equation
def dgl(y,t,k25,k52,k57,k75,k34,k43,k46,k64,k12,k21,k23,k32,k45,k54,k67,k76):
        z1,z2,z3,z4,z5,z6 = y
        dydt = [ -z1*k12+z2*k21, \
                z2*(-k21-k23-k25)+z1*k12+k32*z3+k52*z5, \
                (-k32-k34)*z3+k23*z2+k43*z4, \
                (-k43-k45-k46)*z4+k34*z3+k54*z5+k64*z6, \
                (-k52-k54-k57)*z5+k25*z2+k45*z4+k75*(1-z1-z2-z3-z4-z5-z6), \
                (-k64-k67)*z6+k46*z4+k76*(1-z1-z2-z3-z4-z5-z6)]
        return dydt

#initial conditions
y0 = [z10,z20,z30,z40,z50,z60]

# solution of DEQ system
sol = odeint(dgl, y0, t,args=(k25,k52,k57,k75,k34,k43,k46,k64,k12,k21,k23,k32,k45,k54,k67,k76))

#write data to file
fh = open("daten.txt","w")
print("time Z1 Z2 Z3 Z4 Z5 Z6",file=fh)
for i in range(1, tmax):
        print(t[i], sol[:,0][i], sol[:,1][i], sol[:,2][i], sol[:,3][i], sol[:,4][i], sol[:,5][i], file=fh)
fh.close()

print(sol[:,0][tmax-1])
#create fugure
plt.semilogx(t, sol[:,0],label='z1')
plt.semilogx(t, sol[:,1],label='z2')
plt.semilogx(t, sol[:,2],label='z3')
plt.semilogx(t, sol[:,3],label='z4')
plt.semilogx(t, sol[:,4],label='z5')
plt.semilogx(t, sol[:,5],label='z6')
plt.semilogx(t, 1-sol[:,0]-sol[:,1]-sol[:,2]-sol[:,3]-sol[:,4]-sol[:,5],label='z7')
#plt.semilogx(t, sol[:,1]+2*(1-sol[:,0]-sol[:,1]),label='z4+2*z6')
plt.legend(loc='best')
plt.ylabel('occupation probability')
plt.xlabel('time t [s]')
plt.axis([0.01, 1000000, 0, 1])
plt.show()
```